A stochastic realization approach to the efficient simulation of phase screens

Alessandro Beghi, Angelo Cenedese, and Andrea Masiero

Abstract— The phase screen method is a well established approach to take into account the atmospheric turbulence in astronomical seeing. This is of key importance when designing adaptive optics for the new generation telescopes, in particular when there is need to simulate long exposure phase screen sequence. Turbulence is characterised statistically. A novel approach is presented in this paper, to simulate turbulent phase, based on the stochastic realization theory, which allows to take into account the statistics to extend an existing phase screen in time. The method is consistent with recently presented techniques, and presents appealing properties in terms of accuracy in reconstructing the structure function with a consistent saving of memory.

I. INTRODUCTION

The quest for the ultimate frontier has always challenged the human mind, both towards the microscopic world (from the investigation on the atom structure to modern nanotechnologies, biomedical applications, quantum tecnologies) and towards the immense dimensions of the outer space (one example for all is the epic exploration of the solar system throughout the 20th Century, from unmanned missions to human-crewed expeditions [1]). With reference to the latter, one most intriguing idea has always been that of seeing beyond the human eye [2]. Since the ideal resolution of a telescope (that is the capability of discerning two distant light sources) is given by λ/D, with λ being the light wavelength and D the telescope diameter, improvements in space observations were obtained until the 1980s by basically increasing the mirror size in reflecting ground based telescopes, using monolithic mirrors and mechanical control.

The introduction of computer control brought a quantum leap in the design of multiple mirror telescopes, and furthermore, since *power is nothing without control* (resolution power, in this case!), the use of modern control techniques applied to Adaptive and Active Optics has paved the pathway to the construction of the several meter diameter Very Large Telescope (VLT [3]), and the design of a next generation telescopes bearing the strikingly evocative name of Extremely Large Telescopes (ELTs [4]) and OverWhelmingly Large telescopes (OWL [5]).

A. Active and Adaptive Optics

In these systems, the role of control is twofold.

The application of Active Optics technology allows to replace the massive primary mirror with a very thin mirror, or a segmented mirror, which can be kept in the correct shape by actively adjusting an array of actuators behind the mirror itself. The Active Optics system intervenes to preserve the mirror optimal shape against static or slowly varying environmental factors, such as manufacturing errors, gravity due to telescope inclination, wind, thermal effects.

On the other hand, Adaptive Optics operate on a much shorter timescale to compensate for factors that affect the image at faster timescales (1/100th seconds or even less): these are usually caused by the atmosphere and are not easily corrected with primary mirrors, so that Adaptive Optics have been developed for small corrective mirrors and recently for secondary mirrors. Atmospheric distortions affect the astronomical image with blurring: Adaptive Optics tries to correct these effects by measuring the incoming light with a wavefront sensor and consequently acting on a deformable mirror until the image appears sharp.

B. Turbulence

The wavefront signal from a star object to a ground based telescope is distorted along the light path proportionally to the length of the optic path, and depending on the encountered refraction index: because of this, the wavefront detected at the telescope pupil is no more plane.

Turbulence is a nonlinear chaotic process. Turbulent fluctuations in the wind velocities in the upper atmosphere mix layers of differing temperatures, densities, and water vapour content. As a consequence, the refraction index of each level of the atmosphere fluctuates and the wavefront incident on the telescope along an optical path that encounters these fluctuations has spatial and temporal variations in phase and amplitude. Across the diameter of large telescope the phase errors are a few μm and dominate the degradation of spatial resolution.

A possible way to model turbulence in the atmosphere is the Kolmogorov theory [6][7][8] based on a statistical description of the refractive index, temperature, and velocity of the atmosphere. Kolmogorov started from the assumption of a model based on what he described as an energy transfer cascade. He also introduced inner and outer scales: Outer scale is the largest size scale of the turbulent structure and is related to the size of the structure that initiates the turbulence. Inner scale is the smallest scale where turbulent energy starts to dissipate due to viscous friction. Moreover, wind

velocity fluctuations and the motion of turbulent structures are approximately locally homogeneous and isotropic.

The spectrum of the refraction index is well modelled by Kolmogorov theory only in a limited range of frequencies (the so-called inertial range, which is the spatial range between inner and outer scale), and when there is need to extend predictions beyond this regime instead of the Kolmogorov model the Von Karman spectrum is used, which introduces a characteristic parameter called the wavefront outer scale L_0 leading to attenuation of the phase spectrum at low frequencies. This model tends to the Kolmogorov one when the outer scale tends to infinity.

In order to model atmospheric turbulence we make use of the phase screen method. Pictorially, the phase screen is a randomly inhomogeneous thin layer placed along the path of propagation of a wave and affecting the wavefront with a phase perturbation. In doing so, the phase screen introduces a planar perturbation on an horizontal plane, and along the vertical dimension the turbulence effect is modelled through the insertion of a number of screens each contributing to the overall phase perturbation [9].

From what explained it appears how the simulation of such wavefronts is a crucial step in the design of modern Adaptive Optics systems; in particular, some effort is devoted to the generation of atmospheric phase screens for very long exposures.

II. THE PHASE SCREEN SIMULATION PROBLEM

A. Problem Statement

The crucial question is: how do we choose the properties of the phase screen such that it accurately models the atmosphere?

The turbulent phase ϕ is generally described by means of the structure function, which measures the averaged difference between the phase at two points at locations r_1 and r_2 of the wavefront, which are separated by a distance r on the aperture plane (Fig. 1),

$$D_\phi(r) = \left\langle |\phi(r_1) - \phi(r_2)|^2 \right\rangle.$$

The structure function D_ϕ is related to the covariance function $C_\phi(r) = \langle \phi(r_1), \phi(r_2) \rangle$, as:

$$D_\phi(r) = 2 \left(\sigma_\phi^2 - C_\phi(r) \right), \qquad (1)$$

where σ_ϕ^2 is the phase variance.

According to the Von Karman theory, the phase structure function evaluated at distance r is the following [10]:

$$D_\phi(r) = \left(\frac{L_0}{r_0} \right)^{5/3} c \left[\frac{\Gamma(5/6)}{2^{1/6}} - \left(\frac{2\pi r}{L_0} \right)^{5/6} K_{5/6} \left(\frac{2\pi r}{L_0} \right) \right],$$

where $K_.(\cdot)$ is the MacDonald function (modified Bessel function of the third type), Γ is the Gamma function, L_0 is the outer scale, r_0 is a characteristic parameter called the Fried parameter [11], and c is a suitable constant [1].

[1] That is $c = \frac{2^{1/6}\Gamma(11/6)}{\pi^{8/3}} \left[\frac{24}{5} \Gamma(6/5) \right]^{5/6}$.

From the relation between the structure function and the covariance (1), the spatial covariance of the phase between two points at distance r results

$$C_\phi(r) = \left(\frac{L_0}{r_0} \right)^{5/3} \frac{c}{2} \left(\frac{2\pi r}{L_0} \right)^{5/6} K_{5/6} \left(\frac{2\pi r}{L_0} \right). \qquad (2)$$

We indicate with $\phi(u,v)$ a discrete square phase screen of size $m \times m$ pixels, being $1 \leq u, v \leq m$ as seen by the telescope pupil [2].

Without loss of generality we assume that the physical dimension of each pixel is $p_s \times p_s [m^2]$ (therefore the phase screen has a physical size of $D = mp_s$ meters), although the procedure described can be easily extended to the general case of rectangular pixels. The rationale is that the phase screen evolves in time by basically translating over the telescope pupil with characteristic velocity, and the simulation of this dynamics during very long exposures is obtained by generating new columns of ϕ according to the atmospheric turbulence statistics.

In this framework, the phase screen ϕ is treated as a realization of an m-dimensional stochastic process $\mathbf{\Phi} = \{\phi_t : t \in \mathbb{N}\}$ that we assume to be wide-sense stationary. This implies that the mean function $m_\phi(t) = m_\phi(t + \tau), \forall \tau \in \mathbb{N}$ is constant ($m_\phi = 0$, without loss of generality) and the correlation function depends only on the difference between the evaluation points $C_\phi(t_1, t_2) = C_\phi(t_1 + \tau, t_2 + \tau) = C_\phi(t_1 - t_2, 0), \forall \tau \in \mathbb{N}$. Therefore, we consider the tth column of ϕ, ϕ_t (that is $\phi_t = \phi(:,t)$), as the value at time t of the stochastic process in the realization ϕ.
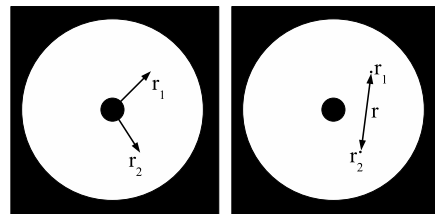

Fig. 1. Two points r_1 and r_2 at distance r on the aperture plane.

B. Stochastic Realization

The stochastic process $\mathbf{\Phi}$ can be also represented as the output y of a linear dynamical system in state space form, that is $y_t = \phi_t$:

$$\begin{cases} x_{t+1} = Ax_t + Ke_t \\ y_t = Cx_t + e_t \end{cases} \qquad (3)$$

where e_t is a zero mean white noise process with covariance matrix $\Sigma_e = \mathbb{E}\left\{ e_t e_t^T \right\} = R$. In (3), the state x and the output y vectors have dimensions respectively n and m, and $A \in \mathbb{R}^{n \times n}$, $K \in \mathbb{R}^{n \times m}$, $C \in \mathbb{R}^{m \times n}$.

The problem of finding a set of parameters $\{A, C, K, R\}$ such that the covariances of the process y_t match a desired

[2] Where u, v are the Cartesian coordinates of a point on the square that inscribes the aperture plane.

covariance matrix Σ_y is called a *stochastic realization problem* [12][15][16][17][18][19][13][14].

Obviously, in the specific phase screen case, the covariance of the stochastic process $\mathbf{\Phi}$ is uniquely determined by the theoretical covariances given by (2).

We define Λ_i as the expected value of the product between two output samples y_{t+i} and y_t, $\Lambda_i = \mathbb{E}\left\{y_{t+i}y_t^T\right\}$, $i = 1, \cdots, 2\nu-1$, where ν is a design parameter in the procedure. From the structure of the model (3), the calculation of the square matrices $\{\Lambda_i\}$ gives the following:

$$\begin{cases} \Lambda_1 = CG \\ \Lambda_2 = CAG \\ \vdots \\ \Lambda_{2\nu-1} = CA^{2\nu-2}G \end{cases} \tag{4}$$

where $G = A\Sigma C^T + KR$, and $\Sigma = \mathbb{E}\left\{x_t x_t^T\right\}$.

Furthermore, a commonly agreed assumption considers that the phase screen translates in front of the telescope pupil with constant velocity [20]. Being η the space traveled in a sample period (proportional to the translation velocity), the values of Λ_i are simply obtained from the covariance function (2), recalling the zero-mean assumption for ϕ_t. In other words:

$$\begin{aligned} \Lambda_i &= \mathbb{E}\left\{y_{t+i}y_t^T\right\} \\ &= \mathbb{E}\left\{(\phi_{t+i} - m_\phi)(\phi_t - m_\phi)^T\right\} = C_\phi(i\eta). \end{aligned}$$

The Λ_i are used to construct the following Hankel matrix (of size $\nu m \times \nu m$):

$$\begin{aligned} H &:= \begin{bmatrix} \Lambda_1 & \Lambda_2 & \cdots & \Lambda_\nu \\ \Lambda_2 & \Lambda_3 & \cdots & \Lambda_{\nu+1} \\ \vdots & \vdots & \ddots & \vdots \\ \Lambda_\nu & \Lambda_{\nu+1} & \cdots & \Lambda_{2\nu-1} \end{bmatrix} \tag{5} \\[2mm] &= \begin{bmatrix} CG & CAG & \cdots & CA^{\nu-1}G \\ CAG & CA^2G & \cdots & CA^\nu G \\ \vdots & \vdots & \ddots & \vdots \\ CA^{\nu-1}G & CA^\nu G & \cdots & CA^{2\nu-2}G \end{bmatrix} \tag{6} \\[2mm] &= \begin{bmatrix} C \\ CA \\ \vdots \\ CA^{\nu-1} \end{bmatrix} \begin{bmatrix} G & AG & \ldots & A^{\nu-1}G \end{bmatrix}. \tag{7} \end{aligned}$$

Conversely, the H matrix can be factorized according to the Singular Value Decomposition algorithm:

$$H = USV^T = US^{1/2}S^{1/2}V^T, \tag{8}$$

with U, V unitary matrices, and S is a diagonal matrix whose elements are the singular values of H. Hence, by comparing (7) with (8), two matrices Ω and $\bar{\Omega}$ can be introduced to obtain $H = \Omega\bar{\Omega}$:

$$\begin{aligned} \Omega &:= US^{1/2} = \begin{bmatrix} C \\ CA \\ \vdots \\ CA^{\nu-1} \end{bmatrix} \\ \bar{\Omega} &:= S^{1/2}V^T = \begin{bmatrix} G & AG & \ldots & A^{\nu-1}G \end{bmatrix}. \end{aligned}$$

Note: the size of Ω and $\bar{\Omega}$ are respectively $\nu m \times n$ and $n \times \nu m$.

In a practical application of the method, most of the singular values of H will be close to zero (Fig. 2), therefore we can use the factorization of H even as a dimensional reduction step considering only the first $\bar{n}$ singular values and setting the other ones to 0:

$$H \approx U_{\bar{n}}S_{\bar{n}}V_{\bar{n}}^T = U_{\bar{n}}S_{\bar{n}}^{1/2}S_{\bar{n}}^{1/2}V_{\bar{n}}^T = \Omega_{\bar{n}}\bar{\Omega}_{\bar{n}} \tag{9}$$

where

$$\begin{cases} U_{\bar{n}} = U(:, 1:\bar{n}) \\ S_{\bar{n}} = S(1:\bar{n}, 1:\bar{n}) \\ V_{\bar{n}} = V(:, 1:\bar{n}) \end{cases}.$$

In this case, the following approximate relations stand:

$$\Omega_{\bar{n}} \approx \begin{bmatrix} C \\ CA \\ \vdots \\ CA^{\nu-1} \end{bmatrix} \tag{10}$$

$$\bar{\Omega}_{\bar{n}} \approx \begin{bmatrix} G & AG & \ldots & A^{\nu-1}G \end{bmatrix}. \tag{11}$$
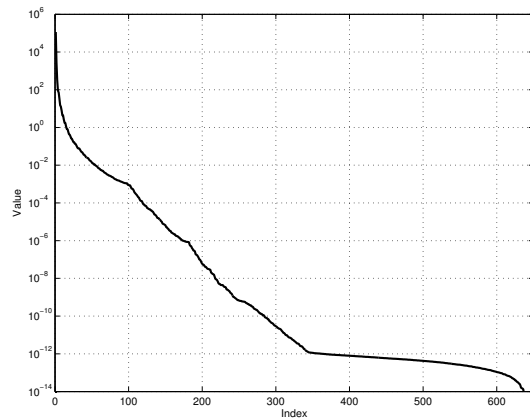

Fig. 2. Plot of the singular values of the stochastic realization model. In the case $\nu = 10$, $m = 64$, hence the size of the A matrix before the reduction step (and the number of the singular values) is $\nu m = 640$.

The solution to the stochastic realization problem is then straightforward. The determination of C and G can be done by inspection from (10)-(11), since:

$$\begin{aligned} C &\approx \Omega_{\bar{n}}(1:m, :) \\ G &\approx \bar{\Omega}_{\bar{n}}(:, 1:m) \end{aligned}$$

Also, A can be computed via least squares from (10)-(11): defining

$$\Omega_u = \Omega_{\bar{n}}(1:(\nu-1)m, :) \approx \begin{bmatrix} C \\ CA \\ \vdots \\ CA^{\nu-2} \end{bmatrix}$$

$$\Omega_d = \Omega_{\bar{n}}(m+1:\nu m, :) \approx \begin{bmatrix} CA \\ CA^2 \\ \vdots \\ CA^{\nu-1} \end{bmatrix}$$

then

$$\Omega_d \approx \Omega_u A \Rightarrow A \approx \Omega_u^{-L}\Omega_d,$$

where $(\cdot)^{-L}$ indicates the left-inverse operator.

From the system equations (3) it is possible to write the time evolution of $\Sigma_t = \mathbb{E}\left\{x_t x_t^T\right\}$:

$$\Sigma_{t+1} = A\Sigma_t A^T + (G - A\Sigma_t C^T)R^{-1}(G - A\Sigma_t C^T)^T,$$

and the steady state covariance matrix Σ is obtained by solving the following Algebraic Riccati Equation (ARE):

$$\Sigma = A\Sigma A^T + (G - A\Sigma C^T)(\Lambda_0 - C\Sigma C^T)^{-1}(G^T - C\Sigma A^T), \tag{12}$$

where the input noise covariance R is computed explicitly from $\Lambda_0 - C\Sigma C^T$.

Finally, the input gain K in the state equation is given by the Kalman gain: $K = (G - A\Sigma C^T)R^{-1}$.

The dynamical model (3) can be now used to synthesize new realizations of the stochastic process ϕ (or to extend in time an existing one). Indeed, given an initial state x_0, the synthesis of new values of y is obtained by simply generating suitable samples of the input e_t (for example by taking independent samples from $\mathcal{N}(0, R)$) and updating the state and output equations in (3).

To give a flavour of the procedure outcome for the specific astronomical application, an example of such a realization is shown in Fig. 3, where a sequence of phase screen is reported.
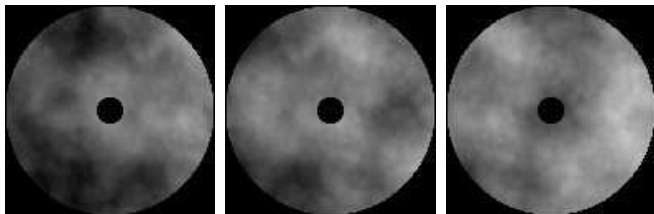

Fig. 3. A sequence of phase screens. The picture serves to give some intuition on how the phase screen actually simulates the presence of a "turbulence pattern" over the telescope pupil.

C. The positivity condition

First let $\{A, C, G\}$ be identified as described in Section II-B and consider the finite covariance sequence:

$$\left\{\bar{\Lambda}_0, \bar{\Lambda}_1, \bar{\Lambda}_2, \dots, \bar{\Lambda}_{2\nu-1}\right\} \tag{13}$$

where the matrices in the sequence are defined as follows

$$\begin{cases} \bar{\Lambda}_0 := \Lambda_0 \\ \bar{\Lambda}_1 := CG \approx \Lambda_1 \\ \bar{\Lambda}_2 := CAG \approx \Lambda_2 \\ \vdots \\ \bar{\Lambda}_{2\nu-1} := CA^{2\nu-2}G \approx \Lambda_{2\nu-1} \end{cases}$$

Then let us consider the infinite sequence

$$\left\{\bar{\Lambda}_0, \bar{\Lambda}_1, \bar{\Lambda}_2, \dots, \bar{\Lambda}_{2\nu-1}, \bar{\Lambda}_{2\nu}, \dots\right\} \tag{14}$$

of $m \times m$ matrices, obtained defining

$$\bar{\Lambda}_i := CA^{i-1}G, \ \forall i \geq 2\nu .$$

The sequence (14) is called a *minimal rational extension*[3] of the finite sequence (13). The matrices of the sequence (14) are supposed to be the covariances of the output process in the dynamical system (3), however note that in general (14) is not a covariance sequence: When (14) is a covariance sequence it is called a *positive sequence*.

Actually, in this case, the main drawback of having identified $\{A, C, G\}$ possibly corresponding to a non-positive sequence is that the Riccati equation (12) may have no solution, so it may be necessary to take a different choice for the state dimension $\bar{n}$ and test again the solvability of the Riccati equation.

However, it is also possible to slightly modify the realization approach of Section II-B to ensure the positivity condition [14].

Let T be the following Toeplitz matrix

$$T = \begin{bmatrix} \Lambda_0 & \Lambda_1 & \Lambda_2 & \cdots & \Lambda_{\nu-1} \\ \Lambda_1^T & \Lambda_0 & \Lambda_1 & \ddots & \Lambda_{\nu-2} \\ \Lambda_2^T & \Lambda_1^T & \Lambda_0 & \ddots & \Lambda_{\nu-3} \\ \vdots & \ddots & \ddots & \ddots & \vdots \\ \Lambda_{\nu-1}^T & \Lambda_{\nu-2}^T & \Lambda_{\nu-3}^T & \cdots & \Lambda_0 \end{bmatrix}$$

and let L be a Cholesky factor of T, that is L is a lower triangular matrix such that $T = LL^T$. Then we define the normalized Hankel matrix as follows

$$\hat{H} := L^{-1}HL^{-T} ,$$

hence

$$H = L\hat{H}L^T. \tag{15}$$

Similarly to what detailed in Section II-B, we factorize $\hat{H}$ using the SVD (again the SVD can be used also as a dimensional reduction step, i.e. considering only the first $\bar{n}$ principal components):

$$\hat{H} \approx U_{\bar{n}}S_{\bar{n}}V_{\bar{n}}^T. \tag{16}$$

So from (15), (16) and since (7) still holds, we can compute C and G as follows:

$$\begin{cases} C \approx \rho_1(H)L^{-T}V_{\bar{n}}S_{\bar{n}}^{-1/2} \\ G \approx (\rho_1(H^T)L^{-T}U_{\bar{n}}S_{\bar{n}}^{-1/2})^T \end{cases} \tag{17}$$

where $\rho_1(\cdot)$ is an operator that selects the first m rows of a matrix.

Furthermore let $\sigma(\cdot)$ be the shift operator, that, applied on the Hankel matrix H, yields

$$\sigma(H) = \begin{bmatrix} \Lambda_2 & \Lambda_3 & \cdots & \Lambda_{\nu+1} \\ \Lambda_3 & \Lambda_4 & \cdots & \Lambda_{\nu+2} \\ \vdots & \vdots & \ddots & \vdots \\ \Lambda_{\nu+1} & \Lambda_{\nu+2} & \cdots & \Lambda_{2\nu} \end{bmatrix}.$$

[3]Note that the minimal rational extension of (13) is uniquely determined by $\{A, C, G\}$.

From (15), (16) and

$$\begin{bmatrix} C \\ CA \\ \vdots \\ CA^{\nu-1} \end{bmatrix} A \begin{bmatrix} G & AG & \dots & A^{\nu-1}G \end{bmatrix} = \sigma(H)$$

we can compute A in the following way:

$$A \approx S_{\bar{n}}^{1/2} U_{\bar{n}}^T L^{-1} \sigma(H) L^{-T} V_{\bar{n}} S_{\bar{n}}^{-1/2} \tag{18}$$

This choice of the matrices $\{A, C, G\}$ can sometimes be more convenient than that of Section II-B, and indeed the following proposition holds.

Proposition 1: Let $\Lambda_i = C_\phi(i\eta)$, $\forall i$ and let A, C, G be computed as in (17) and (18). Then, there is an integer $\nu_1 \geq \nu_0$ such that, for $\nu \geq \nu_1$ then $\{\bar{\Lambda}_0, \bar{\Lambda}_1, \bar{\Lambda}_2, \dots\}$ is a positive sequence.

The proof of Proposition 1 follows straightly from Theorem 5.3 in [14] after introducing the hypotheses that hold here.

D. The "Assemat et al." Method

To validate the method and assess the correctness of the procedure adopted, a recent work by Assémat and colleagues [20] is chosen as a reference. In [20] the problem of extending in time a phase screen of $m \times m$ pixels is considered: This, again, translates into the problem of adding new columns to the phase screen matrix. The solution proposed starts from N "old" phase values piled to form a vector z (of size Nm) and a random input vector β whose components are independent gaussian signals with zero mean and unitary covariance, which are linearly combined in a dynamic relation to form the "new" phase values y:

$$y = Az + B\beta, \tag{19}$$

where A and B are matrices of size $m \times Nm$ and $m \times m$ respectively.

To obtain the system matrices A and B Assémat and coworkers proceed by taking the covariances:

$$\begin{aligned} \Sigma_{yz} &:= \mathbb{E}\{yz^T\} = A\mathbb{E}\{zz^T\} \tag{20} \\ \Sigma_y &:= \mathbb{E}\{yy^T\} = A\mathbb{E}\{zz^T\}A^T + BB^T \tag{21} \end{aligned}$$

From (20), being $\Sigma_z := \mathbb{E}\{zz^T\}$,

$$A = \Sigma_{yz}\Sigma_z^{-1},$$

while from (21)

$$BB^T = \Sigma_y - A\Sigma_z A^T,$$

and hence the B matrix can be obtained resorting to the SVD algorithm.

This approach can be revisited as a particular case of the stochastic realization problem. By assuming the notation of Section II-B, ϕ_t (y in (19)) is considered as the output y_t of the following dynamical model, and the state x_t is obtained by piling the vectors $\{\phi_t, \phi_{t-1}, \dots, \phi_{t-\nu+1}\}$:

$$\begin{cases} x_{t+1} = Ax_t + Bw_t \\ y_t = Cx_t \end{cases} \tag{22}$$

where w_t is a white noise process with unitary covariance. Being m be the dimension of the output and $n = \nu m$ the state dimension is, the process matrices $A \in \mathbb{R}^{n \times n}$, $B \in \mathbb{R}^{n \times m}$, and $C \in \mathbb{R}^{m \times n}$ take the form:

$$\begin{aligned} A &= \begin{bmatrix} \tilde{A}_1 & \tilde{A}_2 \\ I_{(\nu-1)m} & 0 \end{bmatrix} = \begin{bmatrix} \tilde{A} \\ I_{(\nu-1)m} & 0 \end{bmatrix}; \\ B &= \begin{bmatrix} \tilde{B} \\ 0 \\ \vdots \\ 0 \end{bmatrix}; \\ C &= \begin{bmatrix} I_m & 0 & \dots & 0 \end{bmatrix}, \end{aligned}$$

noting that for the sake of simplicity the first m rows of A can be compacted in the $m \times n$ matrix $\tilde{A}$, and B is partitioned accordingly (being $\tilde{B}$ of size $m \times m$).

Let the output covariances Λ_i be defined as in (4), then the state covariance matrix Σ is

$$\Sigma = \begin{bmatrix} \Lambda_0 & \Lambda_1 & \dots & \Lambda_{\nu-1} \\ \Lambda_1 & \Lambda_0 & \dots & \Lambda_{\nu-2} \\ \vdots & \vdots & \ddots & \vdots \\ \Lambda_{\nu-1} & \Lambda_{\nu-2} & \dots & \Lambda_0 \end{bmatrix}.$$

As suggested in [20], $\tilde{A}$ can easily be computed via least squares:

$$\tilde{A} = \begin{bmatrix} \Lambda_1 & \Lambda_2 & \dots \Lambda_\nu \end{bmatrix} \Sigma^{-1}.$$

Moreover, since the process is assumed to be stationary, introducing matrix $Q := \tilde{B}\tilde{B}^T$

$$\begin{aligned} \Sigma &= A\Sigma A^T + BB^T \\ &= \begin{bmatrix} \tilde{A} \\ I_{(\nu-1)m} & 0 \end{bmatrix} \Sigma \begin{bmatrix} \tilde{A}^T & I_{(\nu-1)m} \\ & 0 \end{bmatrix} + \begin{bmatrix} Q & 0 \\ 0 & 0 \end{bmatrix} \end{aligned}$$

thus $Q = \Lambda_0 - \tilde{A}\Sigma\tilde{A}^T$. $\tilde{B}$ (hence, B) can be computed from Q, for example via SVD.

The synthesis process is substantially the same described previously in Section II-B.

III. SIMULATIONS AND DISCUSSION

To begin with, we stress the fact that the methods described can be successfully employed if the (wide sense) stationarity assumption on the process ϕ stands. Furthermore, the synthesis process requires the A matrix in the identified model to be asymptotically stable: The procedure of Section II-C ensures it, while this is general not true for that in [20] (Section II-D).

Two more observations are now in order. First of all, the amount of memory storage necessary for the synthesis of new phase values ϕ_t is that required for storing the matrices $\{A, C, K, R\}$ for the dynamic model (3) and the system state x_t. Since the matrix dimensions depend on the size n of the state vector, it is understandable how it is critical to keep the state dimension quite small. To be more precise: Let n_s and n_a be respectively the state dimensions for procedures of Section II-B (or II-C) and II-D, then the memory required by the two procedures is respectively: $2n_s^2 + n_s m + n_s$ and $2n_a^2 + n_a$. Since $n_a = Nm$ and in our simulations $n_s < m$, then

the stochastic realization approach requires approximatively $\frac{2}{3}N^2$-times less memory than the model by Assémat and colleagues. Similar considerations can be done also for the computational complexity of two algorithms.

Secondly, the parameter ν in both models (3) and (22) corresponds to the number of covariances used in the model identification step: Large values of ν leads to better approximations of the dynamic behavior of the process. Therefore, it would be sensible to choose a large value of ν.

As far as the comparison between the stochastic realization approach (Section II-B,II-C) and the original approach in [20] (Section II-D) is concerned, we observe that the state vector in the model (22) is $n = \nu m$: The state dimension grows linearly with ν, therefore there is a trade-off between the two issues mentioned before. For the state vector to show reasonable dimension, the ν parameter has to be kept small, and indeed, in [20] it is $1 \leq \nu \leq 4$.

Conversely, one main advantage of the approach outlined in Section II-B,II-C is that we can choose n and ν separately and, thanks to the dimension reduction step in the SVD factorization of H in (8), the state dimension $\bar{n}$ will result smaller than νm.

The results reported in [20] refer to typically small values for ν. On the other hand, the beneficial use of the stochastic realization approach should be more evident when the method of [20] fail, that is when there is need for larger ν values. To better clarify this point, we make the following considerations: firstly, the covariance is a decreasing function of r, thus the faster it decreases the smaller ν can be taken (meaning that few sample covariances are necessary to identify the model). Secondly, it can happen that even if ν is small the covariances corresponding to the model of [20] still (approximatively) match the true ones, that is $C\tilde{A}^i \Sigma C^T \approx \Lambda_i$, $i > \nu$.

Finally, we report here some examples of the application of the method proposed, comparing the results with those obtained using the method of [20].

We have to stress that astronomers need phase screen simulations that reconstruct with high accuracy the theoretical statistics of the turbulence and that the structure function for hypothesis is spatially isotropic. Furthermore, since for construction both the method of [20] and the stochastic realization approach preserve the original statistics (almost perfectly) along the vertical direction (see Fig. 4(a)), most of the following examples will show the results along the horizontal direction to verify the isotropic property of the structure function.

The results reported in Fig. 4 are obtained setting the values of the parameters to $L_0 = 20$m, $r_0 = 8$m, $D = 16$m, $p_s = 0.25$m. For the method of [20], $\nu = 2$ and the corresponding dimension of the state is 128. Using the procedure of Section II-B (that of Section II-C would take to similar results) $\nu = 10$, and the state dimension is $n = 60$. We highlight that the model (3), with the parameters identified as in Section II-B, has a much smaller state with respect to that of the model of [20] (60 instead of 128), however, it is evident how its output allows to obtain better
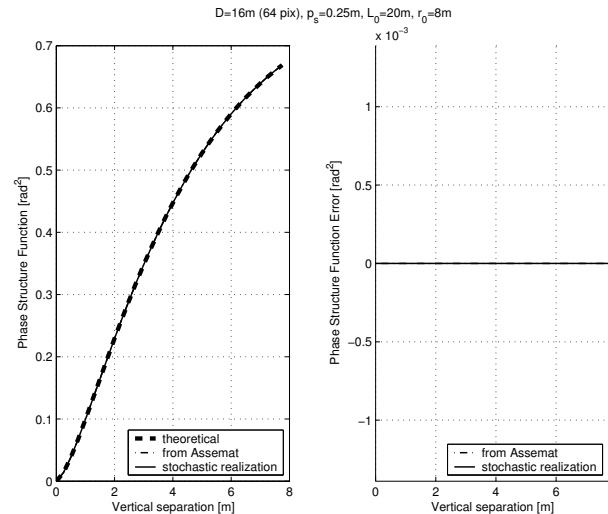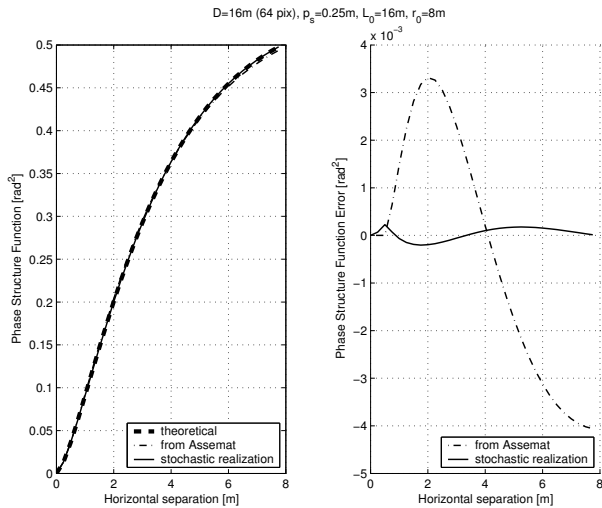

(a)
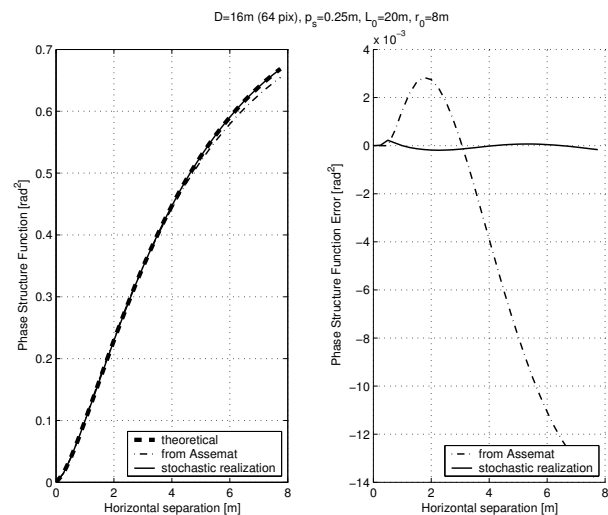
(b)

Fig. 4. In solid line the theoretical phase structure function, in dashed and in dash-dotted lines those obtained with the dynamical model of Section II-B and the method of [20], respectively.

results in terms of estimation of the structure function, thanks to the larger value of ν.

To conclude, we also explore the operative range of the models produced with different turbulence conditions, by varying the outer scale parameter L_0 (basically, the size of the largest turbulence structure) and the Fried parameter r_0 (length-scale over which the turbulence becomes significant) (Figs. 5-6).
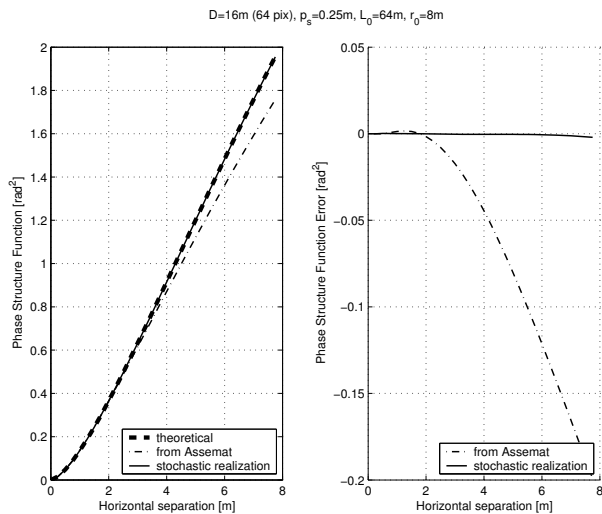
IV. CONCLUSIONS

In this paper we have presented a new framework to develop a dynamic model used to extend phase screen for astronomical applications.
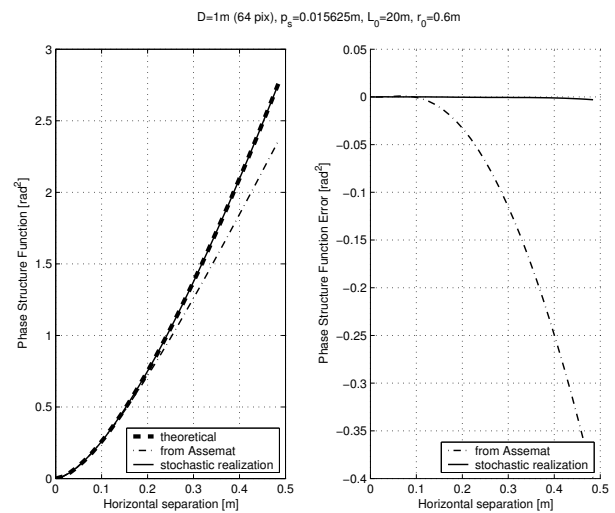
(a)
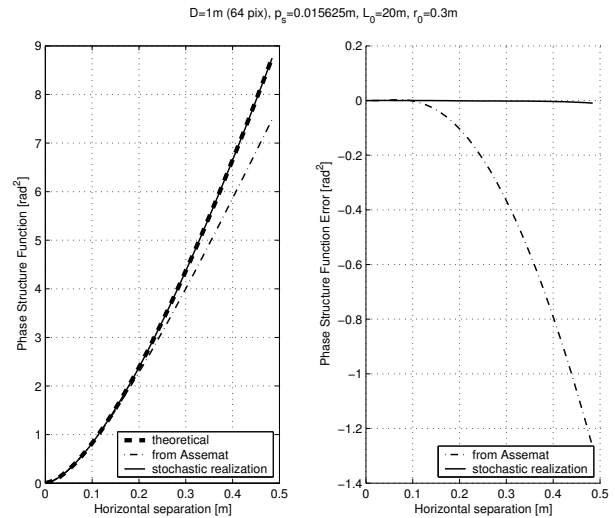
(a)

(b)

(b)

Fig. 5. In solid line the theoretical phase structure function, in dashed and in dash-dotted lines those obtained with the dynamical model of Section II-B and the method of [20], respectively. Different values for the outer scale L_0 are explored: $L_0 = 16m$ (a), $L_0 = 64m$ (b).

Fig. 6. In solid line the theoretical phase structure function, in dashed and in dash-dotted lines those obtained with the dynamical model of Section II-B and the method of [20], respectively. Different values for the Fried parameter r_0 with a telescope diameter $D = 1m$ are explored: $r_0 = 0.3m$ (a), $r_0 = 0.6m$ (b).

On the one hand, we have shown how the stochastic realization approach is consistent with previous work by other scientists, in that the model by Assémat and colleagues is re-interpreted in the general framework proposed.

On the other hand, the model produced using the stochastic realization shows appealing properties of compactness, since the state dimension results much smaller than the correspondent one in [20], and at the same time provides better results in terms of the reconstructed structure function.

V. ACKNOWLEDGMENTS

We are pleased to acknowledge the colleagues of the ELT Project, in particular Ms. Clémentine Béchet and Dr. Michel Tallon at CRAL-Lyon, and Dr. Enrico Fedrigo at ESO-Munich, for their precious help in supporting us with the astronomical view of the problem, and for many valuable and enjoyable discussions on the subject.

REFERENCES

[1] "Space exploration", from Wikipedia, the free encyclopedia [Online], 2006. Available at http://en.wikipedia.org/wiki/Space_exploration
[2] "Telescopes in History", from the Encyclopedia of Astronomy and Astrophysics, Nature Publishing Group, Basingstoke (UK), and Institute of Physics Publishing, Bristol (UK), 2001.
[3] "The Very Large Telescope Project", from the ESO website [Online], 2006. Available at http://www.eso.org/projects/vlt/

[4] M.Le Louarn, N.Hubin, M.Sarazin, and A.Tokovinin, "New challenges for Adaptive Optics: extremely large telescopes" Mon. Not. R. Astron. Soc., vol. 317, pp. 535–544, 2000.

[5] P.Dierickx, J.L.Beckers, E.Brunetto, *et al.* "The eye of the beholder: designing the OWL" Proceedings of SPIE – Future Giant Telescopes, J. Roger P. Angel, Roberto Gilmozzi, Editors, vol. 4840, pp. 151–170, 2003.

[6] A.N.Kolmogorov, "Dissipation of energy in the locally isotropic turbulence", Comptes rendus (Doklady) de l'Acadmie des Sciences de l'U.R.S.S., vol. 32, pp. 16–18, 1941.

[7] A.N.Kolmogorov, "The local structure of turbulence in incompressible viscous fluid for very large Reynold's numbers", Comptes rendus (Doklady) de l'Acadmie des Sciences de l'U.R.S.S., vol. 30, pp. 301–305, 1941.

[8] V.I.Tatarski, *Wave Propagation in a Turbulent Medium*, McGraw-Hill, 1961.

[9] H.G.Booker, T.A.Ratcliffe, and D.H.Schinn, "Diffraction from an irregular screen with applications to ionospheric problems", Phil. Trans. Roy. Soc. A, vol. 242, pp. 579-609, 1950.

[10] R.Conan, "Modélisation des effets de l'échelle externe de cohérence spatiale du front d'onde pour l'observation à Haute Résolution Angulaire en Astronomie", PhD thesis, Université de NiceSophia Antipolis Faculté des Sciences, 2000.

[11] D.L.Fried, "Statistics of a Geometric Representation of Wavefront Distortion", J. Opt. Soc. Am., vol. 55,pp. 1427-1435, 1965.

[12] M.Aoki, *State Space Modeling of Time Series*, 2nd edition, Springer-Verlag, 1991.

[13] H.P.Zeiger, and A.J.McEwen, "Approximate linear realization of given dimension via Ho's algorithm", IEEE Trans. Automatic Control. AC-19, p. 153, 1974.

[14] A.Lindquist, and G.Picci, "Canonical correlation analysis, approximate covariance extension, and identification of stationary time series", Automatica, vol. 32(5), pp. 709–733, 1996.

[15] B.L.Ho and R.E.Kalman, "Effective construction of linear state-variable models from input/output functions", Regelungstechnik, vol. 14, pp.545–548, 1966.

[16] S.Y.Kung, "A new identification and model reduction algorithm via singular value decomposition". In Proceedings of the 12th Asilomar Conference on Circuits, Systems and Computers, Pacific Grove, CA, USA, pp. 705–714, 1978.

[17] H.Akaike, "Stochastic theory of minimal realization", IEEE Trans. Automatic Control, vol. 19, pp. 667–674, 1974.

[18] H.Akaike, "Markovian representation of stochastic processes by canonical variables", SIAM Journal of Control, vol. 13, pp. 162–173, 1975.

[19] U.B.Desai, and D.Pal, "A realization approach to stochastic model reduction and balanced stochastic realizations", In Proceedings of the IEEE Conference on Decision and Control, Orlando, FL, USA, pp. 1105-1112, 1982.

[20] F.Assémat, R.W.Wilson, and E.Gendron, "Method for simulating infinitely long and non stationary phase screens with optimized memory storage", Optics Express, Vol. 14, No. 3, pp. 988–999, 2006.